British Journal of Pharmacology

DOI:10.1111/j.1476-5381.2011.01210.x
www.brjpharmacol.org

RESEARCH PAPER

Rosiglitazone inhibits $K_v4.3$ potassium channels by open-channel block and acceleration of closed-state inactivation

I Jeong[1], BH Choi[2] and SJ Hahn[1]

[1]*Department of Physiology, Medical Research Centre, College of Medicine, The Catholic University of Korea, Seoul, Korea, and* [2]*Department of Pharmacology, Institute for Medical Science, Chonbuk National University Medical School, Jeonju, Jeonbuk, Korea*

Correspondence
Sang June Hahn, Department of Physiology, College of Medicine, The Catholic University of Korea, 505 Banpo-dong, Socho-gu, Seoul 137-701, Korea. E-mail: sjhahn@catholic.ac.kr

Keywords
$K_v4.3$; rosiglitazone; open channel block; closed-state inactivation; PPARγ; type 2 diabetes

Received
6 August 2010
Revised
25 October 2010
Accepted
1 November 2010

BACKGROUND AND PURPOSE

Rosiglitazone is a widely used oral hypoglycaemic agent, which improves insulin resistance in type 2 diabetes. Chronic rosiglitazone treatment is associated with a number of adverse cardiac events. The present study was designed to characterize the effects of rosiglitazone on cloned $K_v4.3$ potassium channels.

EXPERIMENTAL APPROACH

The interaction of rosiglitazone with cloned $K_v4.3$ channels stably expressed in Chinese hamster ovary cells was investigated using whole-cell patch-clamp techniques.

KEY RESULTS

Rosiglitazone decreased the currents carried by $K_v4.3$ channels and accelerated the current inactivation, concentration-dependently, with an IC_{50} of 24.5 μM. The association and dissociation rate constants for rosiglitazone were 1.22 $\mu M^{-1} \cdot s^{-1}$ and 31.30 s^{-1} respectively. Block by rosiglitazone was voltage-dependent, increasing in the voltage range for channel activation; however, no voltage dependence was found in the voltage range required for full activation. Rosiglitazone had no effect on either the deactivation kinetics or the steady-state activation of $K_v4.3$ channels. Rosiglitazone shifted the steady-state inactivation curves in the hyperpolarizing direction, concentration-dependently. The K_i for the interaction between rosiglitazone and the inactivated state of $K_v4.3$ channels was 1.49 μM, from the concentration-dependent shift in the steady-state inactivation curves. Rosiglitazone also accelerated the kinetics of the closed-state inactivation of $K_v4.3$ channels. Rosiglitazone did not affect either use dependence or recovery from inactivation of $K_v4.3$ currents.

CONCLUSION AND IMPLICATIONS

Our results indicate that rosiglitazone potently inhibits currents carried by $K_v4.3$ channels by interacting with these channels in the open state and by accelerating the closed-state inactivation of $K_v4.3$ channels.

LINKED ARTICLE

This article is commented on by Hancox, pp. 496–498 of this issue. To view this commentary visit http://dx.doi.org/10.1111/j.1476-5381.2011.01281.x

Abbreviations

CHO, Chinese hamster ovary cell; K_{ATP} channels, ATP-activated K^+ channels; K_v, voltage-gated K^+ channel; PPARγ, peroxisome proliferator-activated receptor γ.

Introduction

Rosiglitazone, a thiazolidinedione derivative, is a hypoglycaemic agent that is widely used to treat patients with type 2 diabetes. Although its mechanism of action is not fully understood, rosiglitazone is a well-known, high-affinity ligand of the peroxisome proliferator-activated receptor γ (PPARγ; receptor and channel nomenclature follows

Alexander *et al.*, 2009), which increases the insulin sensitivity in peripheral insulin-sensitive tissues (Lehmann *et al.*, 1995; Wagstaff and Goa, 2002). In addition to its antidiabetic effects, rosiglitazone exerts anti-inflammatory, anti-athelosclerotic and anticancer effects, as well direct cardiovascular effects. These effects suggest that rosiglitazone has therapeutic potential beyond treatment of diabetes (Fujiwara and Horikoshi, 2000). However, rosiglitazone directly affects several types of ion channels in cardiovascular muscle cells, independent of PPARγ activation. For example, rosiglitazone reduced voltage-gated L-type Ca^{2+} currents in rat aorta cells and inhibited delayed-rectifier K^+ currents in rat pulmonary arterial myocytes (Knock *et al.*, 1999). Rosiglitazone also inhibited glibenclamide-sensitive K^+ current in isolated rat aorta myocytes (Mishra and Aaronson, 1999). In addition, rosiglitazone abolished shortening of the monophasic action potential in response to an opener of ATP-activated K^+ channels (K_{ATP}) in pig ventricular myocytes, suggesting K_{ATP} channel blockade by rosiglitazone (Lu *et al.*, 2008). We previously reported that rosiglitazone potently inhibited K_v1.3 channels in a manner consistent with an open channel block (Ahn *et al.*, 2007).

The K_v4.3 channel is a member of the *Shal* type of voltage-gated K^+ channels and is highly expressed in the heart and brain (Ohya *et al.*, 1997). The current carried by this channel is a major contributor to cardiac transient outward K^+ currents in human atrial and ventricular myocardium (Dixon *et al.*, 1996). Reduction in K_v4.3 channel activity is commonly observed in conjunction with the prolongation of action potential duration, which seems to be one mechanism of action of antiarrhythmic agents. Thus, K_v4.3 channels are a target of anti-arrhythmia therapies (Wulff *et al.*, 2009). Although no serious cardiac side effects were initially reported, the number of adverse cardiac events, such as heart failure and myocardial infarction, associated with the use of rosiglitazone has increased (Nissen and Wolski, 2007; Singh *et al.*, 2007b). The reduction in transient outward K^+ currents might contribute to prolongation of cardiac action potential duration and ventricular arrhythmia in heart failure and in myocardial infarction (Jeck *et al.*, 1995; Kaab *et al.*, 1998). Because patients with diabetes have a high risk of developing cardiovascular diseases, it is possible that rosiglitazone might cause abnormalities in cardiac electrophysiology, in part, by directly blocking K_v4.3 channels in patients with cardiac disorders. Thus, the purpose of the present study was to characterize the effects of rosiglitazone on K_v4.3 channels and to compare its mechanism of action with that of the effects of rosiglitazone on the delayed rectifier K^+ currents, carried by K_v1.3 channels. Our results suggest that rosiglitazone inhibits K_v4.3 channels by a mechanism that is quite different from that reported for K_v1.3 channels.

Methods

Cell culture

Chinese hamster ovary (CHO) cells stably expressing K_v4.3 channels were used in the present study. The cells were transfected with cDNA encoding K_v4.3 channels using the Lipofectamine reagent (Invitrogen, Grand Island, NY, USA), as described previously (Ahn *et al.*, 2006). The stable cell line expressing K_v4.3 channels was maintained in a humidified atmosphere at 37°C with 5% CO_2-enriched air. Cells were cultured in 50 mL polystyrene culture flasks in Iscove's modified Dulbecco's medium (Invitrogen) supplemented with 10% fetal bovine serum (Invitrogen), 2 mM glutamine (Invitrogen), 0.1 mM hypoxanthine (Invitrogen), 0.01 mM thymidine (Invitrogen), 0.3 $mg \cdot mL^{-1}$ G418 (Invitrogen) and 1% of a 100X antibiotic antimycotic mixture (Invitrogen). Cells were passaged every 2–3 days by brief trypsinization. The cells treated with trypsin-EDTA solution were plated on glass coverslips (12 mm diameter; Fisher Scientific, Pittsburgh, PA, USA) and placed in 35 mm Petri dishes. Patch-clamp recordings were obtained 12–24 h later. For voltage-clamp recordings, the coverslips containing adherent CHO cells were mounted on the glass bottom of the recording chamber (RC-13; Warner Instrument, Hamden, CT, USA) and were perfused with an extracellular bath solution.

Electrophysiological recordings

K_v4.3 channel currents were recorded using the whole-cell configuration of the patch-clamp technique with a glass micropipette connected to an Axopatch 200B patch-clamp amplifier (Molecular Devices, Sunnyvale, CA, USA). All recordings were performed at room temperature (22–24°C). The glass micropipette electrodes were pulled from soft glass capillaries (PG10165-4; World Precision Instruments, Sarasota, FL, USA) using a programmable horizontal microelectrode puller (P-97; Sutter Instrument Co., Novato, CA, USA). The recording pipette tip resistance was typically between 2 and 4 MΩ when filled with the internal solution. Command-voltage generation, data acquisition and data analysis were performed on an IBM-compatible Pentium computer running pClamp 10.0 software (Molecular Devices) using a Digidata 1322A interface (Molecular Devices). After control data were obtained, the perfusion bath was replaced with a drug-containing solution. The liquid junction potential was offset to zero prior to formation of the membrane-pipette seal when the electrode tip was in the bath. After gigaseal formation, gentle suction was applied to rupture the membrane for whole-cell recordings. The sampling frequency was 5 kHz, and the current signals were low-pass filtered at 2 kHz (four-pole Bessel filter) prior to digitization and storage. In the whole-cell configuration, the average series resistance was 3.7 MΩ. The effective series resistances were usually compensated by 80% if the K_v4.3 channel current exceeded 1 nA. Voltage drops, based on the calculated series resistance, were less than 5 mV.

Solutions and drugs

For recording K_v4.3 channel current, the extracellular bath solution, which contained (in mM) 140 NaCl, 5 KCl, 1 $CaCl_2$, 1 $MgCl_2$ and 10 HEPES, was adjusted to pH 7.3 with NaOH. The intracellular pipette-filling solution, which contained (in mM) 140 KCl, 1 $CaCl_2$, 1 $MgCl_2$, 10 HEPES and 10 EGTA, was adjusted to pH 7.3 with KOH. Solutions were applied to the bath with a gravity-fed sewer pipe system. A stock solution of rosiglitazone (Cayman Chemical, Ann Arbor, MI, USA) was initially prepared by dissolving the rosiglitazone in dimethyl

sulfoxide (DMSO). The stock solution was then diluted with the extracellular solution to obtain the desired final concentration.

Data analysis

Data analysis was performed using Origin 8.0 software (Origin Lab Corp., Northampton, MA, USA). The concentration dependence of the current block by rosiglitazone was fitted to the Hill equation, as follows:

$$y = 1/[1 + ([D]/IC_{50})^n]$$

where IC_{50} is the concentration of rosiglitazone required to produce the half-maximum current block, [D] is the rosiglitazone concentration and n is the Hill coefficient. $K_v4.3$ currents were elicited by applying 500 ms depolarizing pulses from a holding potential of –80 to +40 mV, and the interval time under all conditions was 10 s to prevent any aggregation of inactivation or inhibition. The kinetics of interaction between the drug and the channels were described based on a first-order blocking scheme (Snyders and Yeola, 1995). Using this model, the apparent association (k_{+1}) and dissociation (k_{-1}) rate constants were obtained from the following equation:

$$1/\tau_{Block} = k_{+1}[D] + k_{-1}$$

where τ_{Block} is the drug-induced, current decay time constant, and [D] denotes the drug concentration. The voltage dependence of the fractional block was fitted to the Woodhull equation, as follows:

$$f = [D]/\{[D] + K_d(0) \times \exp(-z\delta FV/RT)\}$$

where $K_d(0)$ is the apparent affinity at 0 mV (the reference voltage), z is the charge valence of the drug, δ is the fractional electrical distance (i.e. the fraction of the transmembrane electric field sensed by a single charge at the receptor site), F is Faraday's constant, R is the gas constant and T is the absolute temperature. In the present study, 25.4 mV was used as the RT/F value at 22°C. Steady-state activation curves were derived by normalizing the tail currents measured at –60 mV after the application of 8 ms depolarizing pulses at potentials between –80 and +80 mV in 10 mV increments every 10 s from a holding potential of –80 mV in the absence and presence of rosiglitazone. The following Boltzmann equation was used to fit the data to calculate the steady-state activation:

$$y = 1/\{1 + \exp[-(V - V_{1/2})k]\}$$

where $V_{1/2}$ is the voltage at which the conductance was half-maximal, V is the test potential and k represents the slope of the activation curve. The voltage dependence of steady-state inactivation in the absence and presence of drugs was obtained by normalizing the peak current amplitudes using a two-step, voltage-clamp protocol. The current was produced by a 500 ms depolarizing pulse to +40 mV, whereas 1 s preconditioning pulses were varied from –110 to +10 mV by the increment of 10 mV at 10-s intervals. The curves were fitted to the Boltzmann equation:

$$(I - I_c)/(I_{max} - I_c) = 1/[1 + \exp(V - V_{1/2})k]$$

in which I_{max} represents the current measured at the most hyperpolarized preconditioning pulse, and I_c represents a non-inactivating current at the most depolarized preconditioning pulse. V, $V_{1/2}$ and k are the test potential, the point where channels are half-inactivated, and the slope respectively. The non-inactivating residual current was removed by subtracting it from the actual value. To determine the time course of recovery of the $K_v4.3$ currents from inactivation, a two-pulse protocol was used. The first pre-pulse of a 500 ms depolarizing pulse of +40 mV from a holding potential of –80 mV was followed by a second identical pulse after increasing the inter-pulse intervals between 5 and 10 000 ms at –80 mV. The peak currents elicited during the test pulses were measured and then normalized to the peak currents of the conditioning pulses in the same cell. Normalized recovery data were plotted against the inter-pulse interval and fitted to a single exponential function.

Statistics

Data obtained in the absence and presence of rosiglitazone were analyzed in a paired manner. All averaged and normalized data are summarized as means ± SE. One-way analysis of variance for comparisons of multiple groups followed by Bonferroni's test was used for statistical analysis. Differences were considered significant at $P < 0.05$.

Results

Concentration-dependent block of $K_v4.3$ channels by rosiglitazone

Figure 1A shows the superimposed $K_v4.3$ channel currents that resulted from a 500 ms depolarizing pulse to +40 mV under control conditions and in the presence of rosiglitazone. Under control conditions, the $K_v4.3$ currents were activated to maximum and then were rapidly inactivated as reported previously (Ohya *et al.*, 1997; Ahn *et al.*, 2006; Kim *et al.*, 2007). Rosiglitazone not only reduced the peak amplitude of the $K_v4.3$ currents but also altered the time course of the current decay. At rosiglitazone concentrations up to 10 μM, the peak amplitude of the $K_v4.3$ current was not significantly inhibited, but the rate of current inactivation was accelerated in a concentration-dependent manner. Thus, the concentration-dependent reduction in the $K_v4.3$ current was quantified from the integral of the current during the depolarizing pulse with an IC_{50} of 24.54 ± 1.73 μM and a Hill coefficient of 1.62 ± 0.11 (n = 13) (Figure 1B). At +40 mV, the inactivation of $K_v4.3$ channels was best fit by the sum of two exponentials with a fast (37.0 ± 1.8 ms) and a slow (167.3 ± 7.9 ms, n = 13) component, representing 86.9% and 13.1% of total inactivation respectively. The ratio of the amplitudes of the two components indicates that the inactivation of $K_v4.3$ current was dominated by the fast time constant under control conditions. At 3, 10, 30 and 100 μM, rosiglitazone reduced the fast time constant to 31.8 ± 3.6, 28.9 ± 3.1, 21.2 ± 2.2 and 11.8 ± 1.1 ms and the slow time constant to 140.6 ± 7.2, 132.7 ± 2.9, 123.9 ± 6.7 and 97.9 ± 2.4 ms (n = 13) respectively. However, the relative contribution of the fast component to the total inactivation of the $K_v4.3$ current was not significantly altered (86–72%) by rosiglitazone.

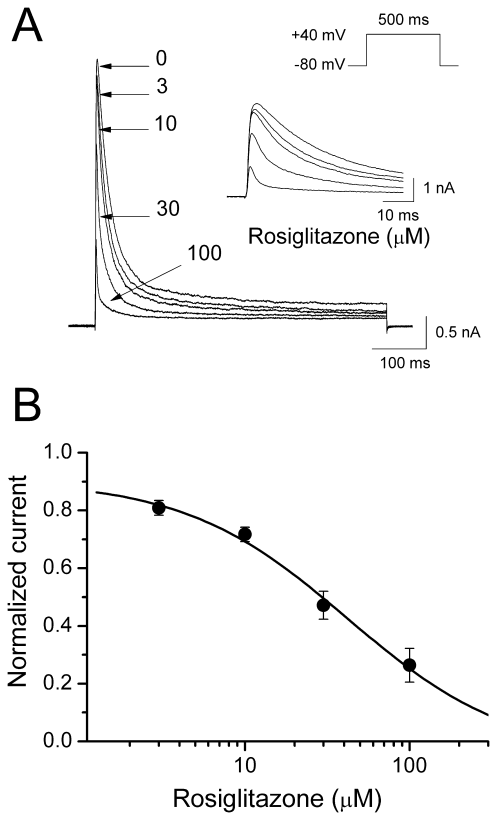

Figure 1

(A) Concentration-dependent effect of rosiglitazone on K_v4.3 channel currents following a 500 ms depolarizing pulse to +40 mV from a holding potential of –80 mV at 10 s intervals. The inset shows the first 50 ms of the current recordings on an expanded time scale. (B) Concentration–response curve for rosiglitazone was fitted to the Hill equation to obtain the IC_{50} value. Data are expressed as means ± SE.

Time-dependent interactions between K_v4.3 channels and rosiglitazone

As shown in Figure 1A, in the presence of rosiglitazone, the decay of K_v4.3 channel current was accelerated in a concentration-dependent manner due to both block by the drug and the intrinsic inactivation of K_v4.3 channels. The time course of rosiglitazone block of K_v4.3 channels was then characterized by subtracting the current in the presence of the drug from the control current (Figure 2A). The time-dependent block of K_v4.3 channels by rosiglitazone was fitted to a biexponential function that yielded the concentration-dependent fast and slow time constants. The time constant of the fast component is a reasonable approximation of the drug–channel interaction kinetics. A plot of the reciprocal of the time constants versus rosiglitazone concentrations yielded an apparent association rate constant (k_{+1}) of 1.22 ± 0.05 $\mu M^{-1} \cdot s^{-1}$ and a dissociation constant (k_{-1}) of 31.30 ± 2.44·s^{-1} (n = 13) (Figure 2B). The estimated K_D (k_{-1}/k_{+1}) was 25.7 ± 2.3 μM, which was in good agreement with the IC_{50} value of 24.5 ± 1.7 μM calculated from the concentration-response curve.

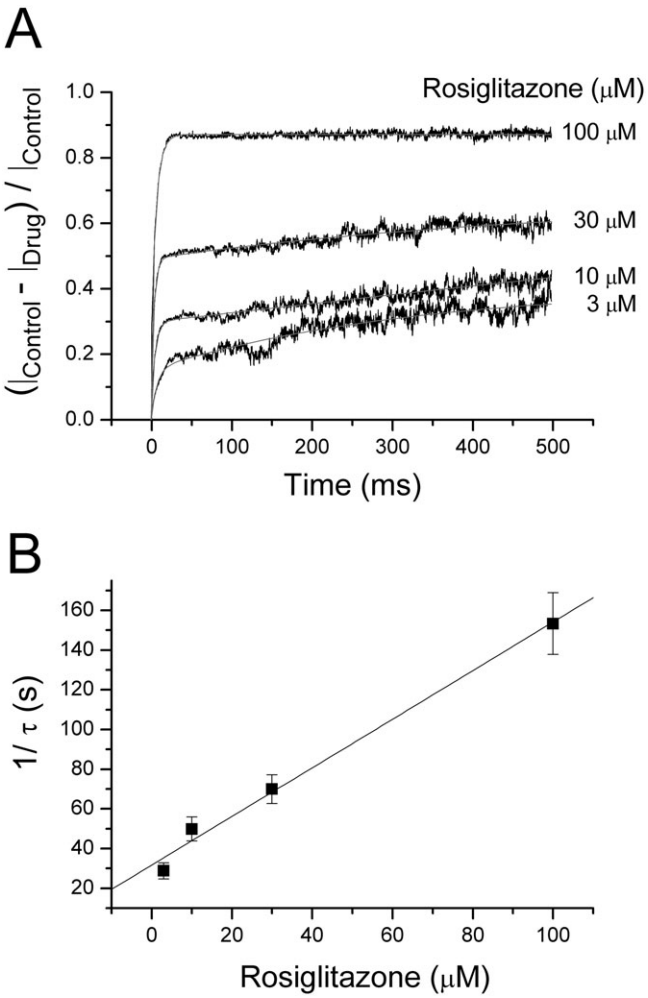

Figure 2

Time-dependent block of K_v4.3 channels by rosiglitazone. (A) The fractional block was calculated by subtracting the ratio of the current before and after addition of the drug from unity. This procedure was carried out at four different drug concentrations. The time courses of inhibition were fit to a biexponential function that yielded the concentration-dependent time constants. (B) The inverse of the fast components of the time constants were plotted against the rosiglitazone concentrations. The solid line represents the least-squares fit of the data to the following equation: $1/\tau_{Block} = k_{+1}[D] + k_{-1}$. Data are expressed as means ± SE.

Voltage-dependent block of K_v4.3 channels

The current–voltage relationships were evaluated in the absence and presence of 30 μM rosiglitazone (Figure 3A,B). K_v4.3 channel currents were generated by depolarizing the cells from a holding potential of –80 mV to a series of a test potentials ranging from –80 to +60 mV and were activated for potentials greater than –30 mV (Figure 3C). The inhibitory effects of rosiglitazone during the depolarizing pulses to different voltages were related to the voltage dependence of activation (Figure 3D). Block was small at –20 mV but increased steeply as the voltage of the pulse became more positive. When the Woodhull equation was applied to data collected at full-activation voltages (above +20 mV), however,

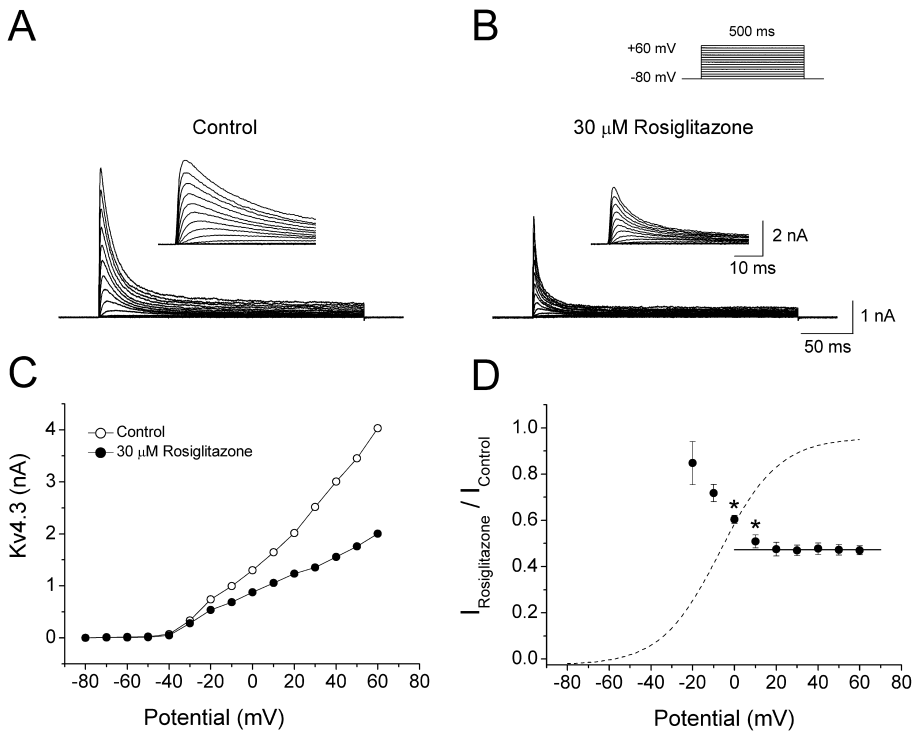

Figure 3

Effect of rosiglitazone on current–voltage relationships. The representative whole-cell $K_v4.3$ channel current traces under control conditions (A) and in the presence of rosiglitazone (B). The inset shows the first 50 ms of the current recordings on an expanded time scale. (C) Current–voltage curves for rosiglitazone-induced $K_v4.3$ currents. The data were taken from the peak amplitude of $K_v4.3$ currents under control conditions and in the presence of rosiglitazone. (D) The integral of the current in the presence of rosiglitazone was normalized to that of the control at each voltage. In the voltage range for channel activation between –20 and +20 mV, the block of $K_v4.3$ channels increased and was significantly different from inhibition at –20 mV (n = 6, *P < 0.05). The dotted line represents the activation curve of $K_v4.3$ channels under control conditions. Data are expressed as means ± SE.

a fractional electrical distance (δ) of 0 was obtained for the binding site of rosiglitazone. This result indicates that there was no effect of the electrical field on the interaction of rosiglitazone with $K_v4.3$ channels.

Effects of rosiglitazone on deactivation kinetics of $K_v4.3$ channels

The tail currents were measured before and after application of rosiglitazone (Figure 4). In the absence of the drug, the $K_v4.3$ currents were completely deactivated at –60 mV with a time constant of 19.61 ± 2.23 ms (n = 7). Rosiglitazone at 3, 10 and 30 μM reduced the amplitude of the tail current in a concentration-dependent manner but did not change the time course for the deactivation of $K_v4.3$ channels. The average values of time constants were 20.64 ± 2.75, 21.37 ± 2.01 and 21.58 ± 1.52 ms (n = 7) for 3, 10 and 30 μM rosiglitazone respectively.

Effects of rosiglitazone on the steady-state activation of $K_v4.3$ channels

The voltage dependence of the steady-state activation of $K_v4.3$ channels was evaluated by tail current analysis with a two-pulse protocol using a series of step depolarizations in

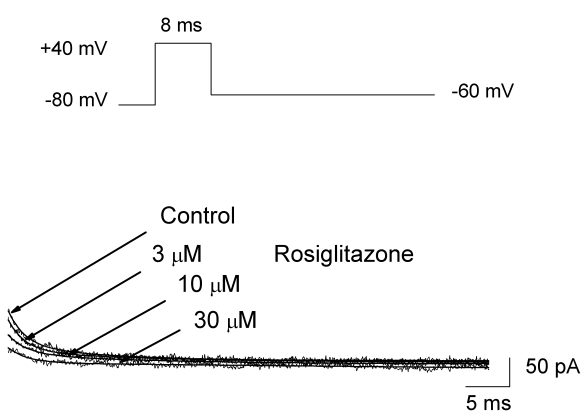

Figure 4

Effect of rosiglitazone on the deactivation kinetics of $K_v4.3$ channels. Tail currents were obtained at –60 mV after 8 ms depolarizing pulses to +40 mV at 10 s intervals in the absence and presence of rosiglitazone. The solid lines represent the single exponential fit and the dotted line represents zero current.

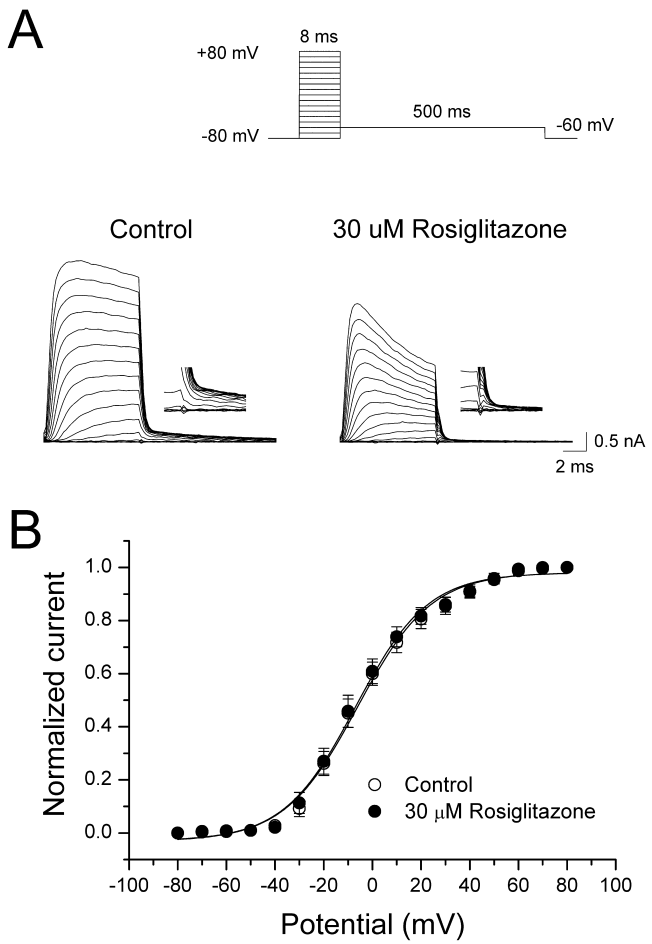

Figure 5

Effect of rosiglitazone on the steady-state activation of K_v4.3 channels. (A) The representative tail current traces of the K_v4.3 channels in the absence and presence of rosiglitazone. The inset shows the tail currents on an expanded time scale. (B) The normalized currents were plotted as a function of the test potentials, and the resulting curves were well fit to the Boltzmann equation. Data are expressed as means ± SE.

the absence and presence of rosiglitazone (Figure 5A). The plot of normalized tail currents followed the Boltzmann distributions (Figure 5B). The potentials for the half-activation point ($V_{1/2}$) and slope (k) of the steady-state activation curve were –13.91 ± 0.91 and 5.65 ± 0.91 mV under control conditions and –14.43 ± 0.78 and 6.48 ± 0.17 mV in the presence of 30 μM rosiglitazone respectively (n = 7). Rosiglitazone slightly shifted the steady-state activation curves towards hyperpolarizing directions, but these values were not statistically different from control values. These results suggest that rosiglitazone did not markedly alter the voltage-dependence of the steady-state activation of K_v4.3 channels.

Effects of rosiglitazone on the steady-state inactivation of K_v4.3 channels

The steady-state curves for inactivation of K_v4.3 channels were generated using a typical two-pulse protocol, in which the 1 s conditioning pulses from a holding potential of –80 mV to potentials between –110 and +10 mV were followed by a test pulse to +40 mV (Figure 6A). The resultant curves were well fitted by the Boltzmann equation to estimate $V_{1/2}$ and k. The steady-state inactivation curves for K_v4.3 in the control condition had a $V_{1/2}$ value of –40.28 ± 0.14 and a k of 4.91 ± 0.11 mV (n = 6). Rosiglitazone significantly shifted the inactivation curve ($V_{1/2}$) towards a hyperpolarized potential in a concentration-dependent manner (–51.71 ± 0.13 mV at 30 μM, –62.68 ± 0.31 mV at 100 μM, n = 6, P < 0.05). However, rosiglitazone had no significant effect on the k of the inactivation curve (4.66 ± 0.13 mV at 30 μM, 4.83 ± 0.28 mV at 100 μM, n = 6). Whereas the IC_{50} value for the rosiglitazone-induced block of K_v4.3 channels in the open state was estimated from the reduction in the integral current of the K_v4.3 channels (Figure 1A), the apparent dissociation constant, K_i, for rosiglitazone-induced inhibition in the inactivated state was estimated from the concentration-dependent shift in the steady-state inactivation curve (Bean *et al.*, 1983). The theoretical value of K_i was calculated to be 1.49 ± 0.12 μM (n = 6) (Figure 6B). Therefore, the affinity of rosiglitazone for the inactivated state of the K_v4.3 channels was increased more than 14-fold relative to that of the open state.

Effects of rosiglitazone on closed-state inactivation of K_v4.3 channels

Because the steady-state inactivation of K_v4.3 channels readily occurs in the closed state (Patel *et al.*, 2004), we determined the effects of rosiglitazone on the kinetics of closed-state inactivation. Closed-state inactivation kinetics was measured using a double-pulse protocol with pulses of progressively increasing duration to a potential of –60 mV below the activation threshold (Figure 7A). The time course for closed-state inactivation was fitted to a single exponential curve with time constants of 4.82 ± 0.26 and 1.51 ± 0.09 s (n = 9) in the absence and presence of 30 μM rosiglitazone respectively (Figure 7B). This result suggests that rosiglitazone accelerates the kinetics of closed-state inactivation of K_v4.3 channels.

Use-independent inhibition of K_v4.3 channels

To assess whether the inhibition of the Kv4.3 channel displays use dependence, the effects of rosiglitazone were evaluated with a series of 10 consecutive 200 ms depolarizing pulses to +40 mV from a holding potential of –80 mV at a frequency of 1 or 2 Hz (Figure 8A). Under control conditions, the peak amplitude of the K_v4.3 channel current during the 10 depolarizing pulses progressively decreased to a steady level and was reduced by 2.32 ± 0.33% and by 19.53 ± 1.69% at 1 and 2 Hz respectively (n = 10) (Figure 8B). In the presence of 30 μM rosiglitazone, the peak amplitude of the K_v4.3 current was not significantly reduced after the first depolarizing pulse in each series, which suggests that the current did not undergo tonic block by the drug. The extent of the steady-state inhibition was 2.70 ± 0.41% at a frequency of 1 Hz and 19.84 ± 1.32% at a frequency of 2 Hz (n = 10). Therefore, the inhibition of the K_v4.3 channel current by rosiglitazone was not use-dependent.

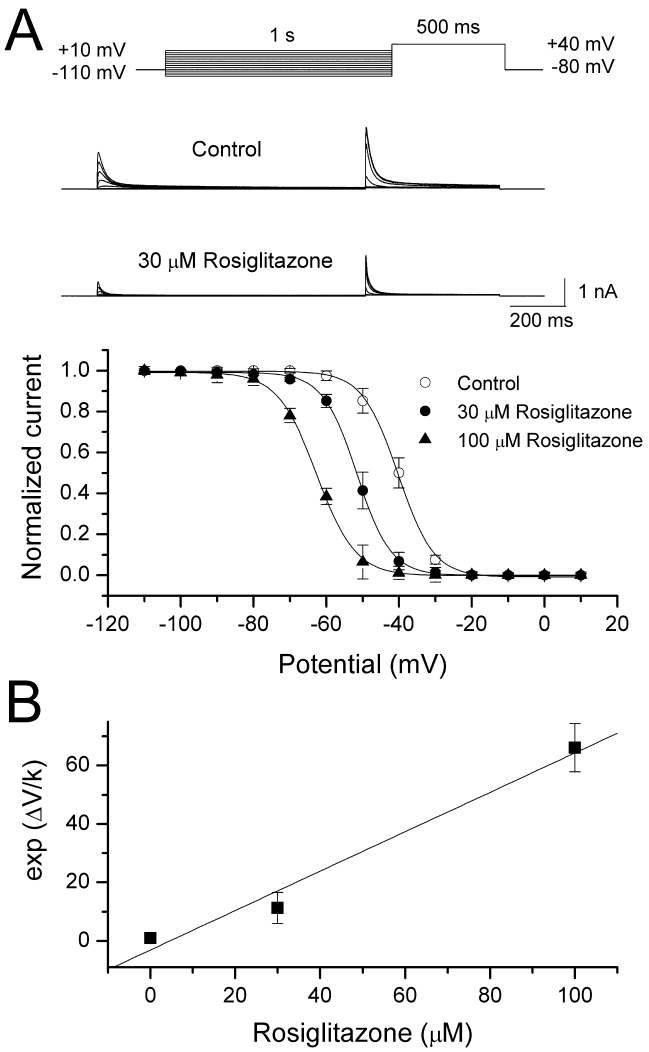

Figure 6

Effect of rosiglitazone on the steady-state inactivation of K_v4.3 channels. (A) Representative K_v4.3current traces in the absence and presence of rosiglitazone were recorded using a two-pulse protocol. Normalized currents of the K_v4.3 channels, which were the currents after the second pulse relative to the current recorded after the first pulse, are shown as a function of the holding potentials. (B) The plot of exp ($\Delta V/k$) against rosiglitazone concentrations. The $V_{1/2}$ and k values were obtained from the steady-state inactivation curves. The concentration-dependent shift in the midpoint (ΔV) was determined as the difference between $V_{1/2}$ values in control conditions and at 30 and 100 μM rosiglitazone ($n = 6$). The affinity of rosiglitazone for the inactivated state of Kv4.3 can be calculated on the basis of this shift: $-\Delta V/k = \ln[(1 + D/K_i)/(1 + D/K_R)]$ where D is the drug concentration, and K_i and K_R are the apparent dissociation constants for the inactivated and resting states respectively (Bean *et al.*, 1983). If one assumes that K_R is very large, the following equation can be used to calculate K_i: $\exp(-\Delta V/k) = D/K_i + 1$. The solid line represents the linear fit of the data: exp ($\Delta V/k$) = 0.67 [rosiglitazone] − 3.09, where [rosiglitazone] represents the rosiglitazone concentration. K_i, the reciprocal of the slope, was calculated from this fit. Data are expressed as means ± SE.

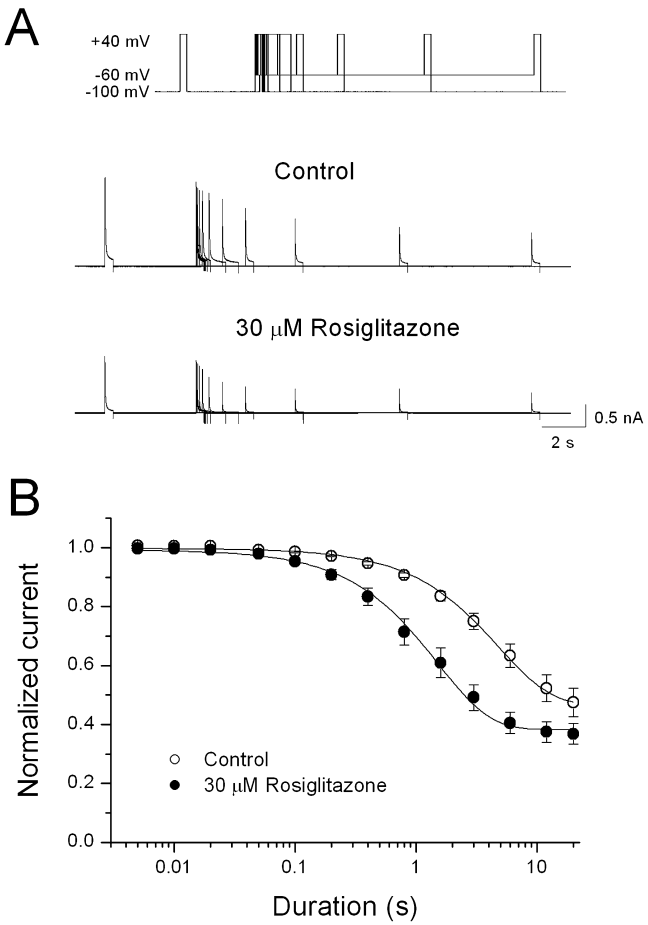

Figure 7

Effects of rosiglitazone on the kinetics of K_v4.3 channels during closed-state inactivation. (A) K_v4.3 currents were recorded at +40 mV using a double-pulse protocol. The control pulse was applied from a membrane potential of −100 mV. (B) The current amplitudes evoked by the second pulse, relative to the amplitude resulting from the initial control pulse, were plotted against the duration of the conditioning pulse. The data were well fit to a single exponential function ($n = 9$). Data are expressed as means ± SE.

Effects of rosiglitazone on the time course of recovery from inactivation of K_v4.3 channels

The time course of recovery from rosiglitazone-induced inhibition of K_v4.3 channels was determined using a double-pulse protocol (Figure 9A). The data for recovery from inactivation of K_v4.3 current were well defined by a single exponential equation in the absence and presence of 30 μM rosiglitazone. The recovery time constant under control conditions was 95.21 ± 1.53 ms, and the time constant for recovery in the presence of rosiglitazone was 98.13 ± 2.10 ms ($n = 6$) (Figure 9B). These results indicate that rosiglitazone has no effect on the recovery from inactivation of K_v4.3 channels.

Discussion

In the present study, the inhibition of K_v4.3 channels by rosiglitazone was characterized by a reduction in peak

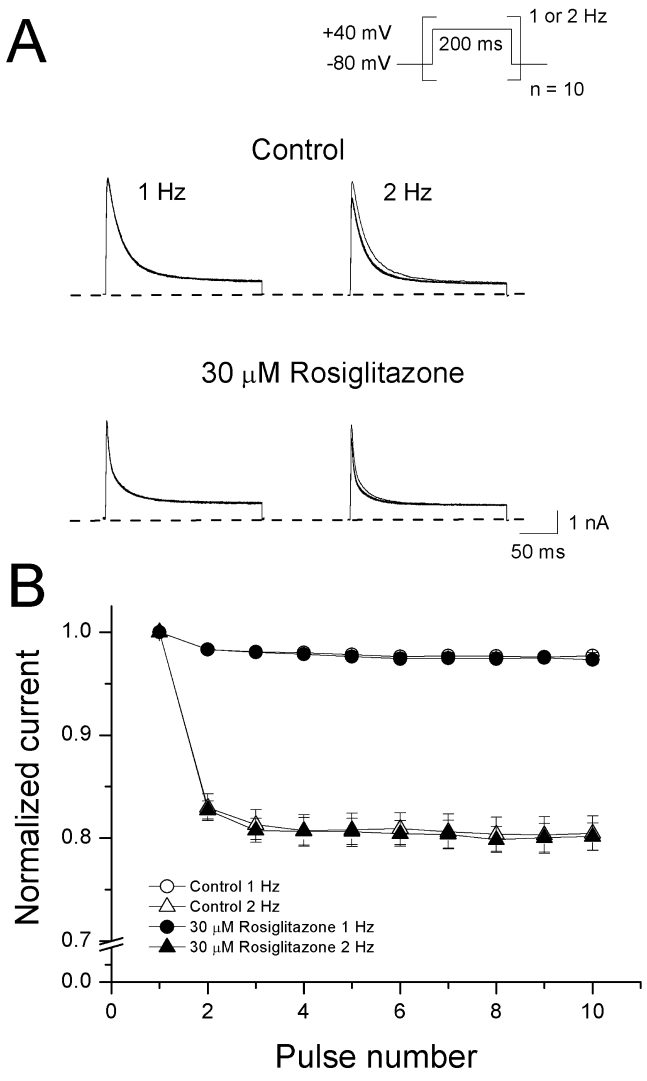

Figure 8

Effect of rosiglitazone on use-dependent inhibition of K_v4.3 channels. (A) K_v4.3 current traces obtained from depolarizing pulses at 1 or 2 Hz in the absence and presence of rosiglitazone. (B) Plot of normalized currents as a function of the number of pulses. The peak amplitudes of the current after each pulse were normalized to the peak amplitude of the current obtained after the first pulse. Data are expressed as means ± SE.

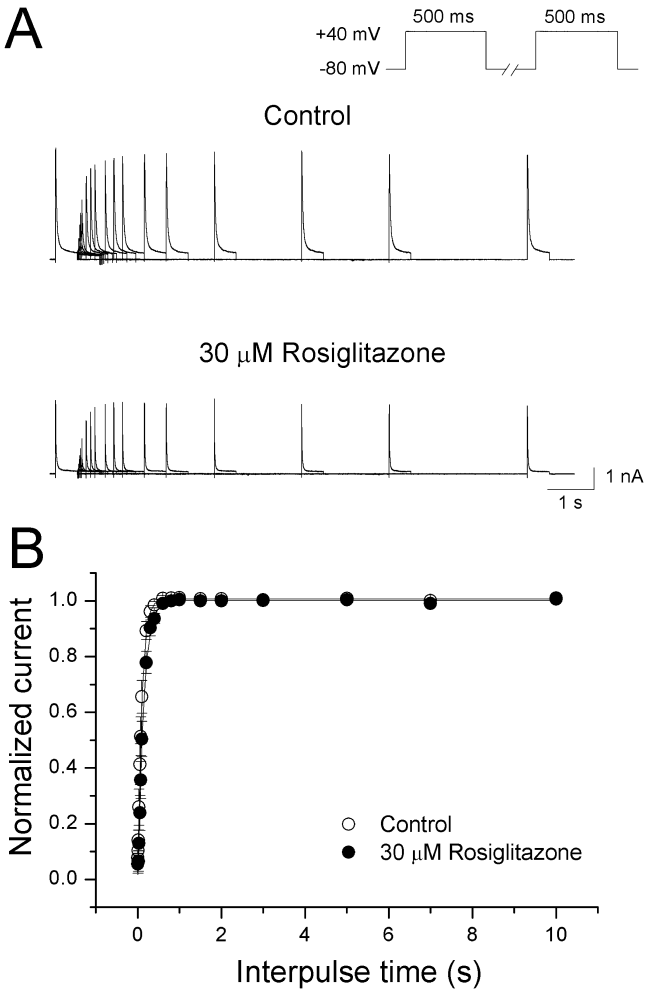

Figure 9

Effects of rosiglitazone on recovery from inactivation of K_v4.3 channels. (A) A double-pulse protocol was used to characterize the recovery of K_v4.3 channels from inactivation in the absence and presence of rosiglitazone. (B) The solid lines represent the single exponential fit of the peak amplitude of the K_v4.3 currents as a function of the interpulse interval. Data are expressed as means ± SE.

amplitude and by an acceleration of the inactivation rate in a concentration-dependent manner. The acceleration in the decay rate of K_v4.3 channel inactivation could be explained by a preferential interaction between rosiglitazone and K_v4.3 channels in the open state or by a drug-induced acceleration in the transition of the open channels to an inactivated state (Wang *et al.*, 1995). There are several similarities between open-channel block and channel inactivation (Demo and Yellen, 1991). The most noticeable effect in our study, however, was the induction of a fast component of current decay during the depolarizing pulse, which was superimposed on the intrinsic inactivation of the K_v4.3 channels. These results suggest that the time course of the channel block that occurred during depolarization was very consistent with the kinetics of a simple model of open-channel block (Snyders and Yeola, 1995). From the analysis of the concentration dependence of the channel block, the estimated K_D (k_{-1}/k_{+1}) value for the time-dependent block by rosiglitazone was similar to the IC_{50} value obtained from the concentration-response curve shown in Figure 1. Thus, these results imply that the effect of rosiglitazone on K_v4.3 channels was independent of the inactivation process and was classified as open-channel block. Furthermore, the exponential curve fits, which were extrapolated to zero at the start of the depolarization, indicate that the onset of the channel block occurred after channel activation. In addition, voltage dependence is indicative of enhanced current block in response to increasing membrane depolarization. This phenomenon has also been observed in open-channel block (Snyders *et al.*, 1992; Wang *et al.*, 1995). The block of the

K_v4.3 channels by rosiglitazone increased with channel opening over the voltage range of activation. This result suggests an interaction with channels in the open state, but the block of K_v4.3 channels in the full activation range showed no voltage dependence. These findings are consistent with those reported for the block of K_v1.3 channels by rosiglitazone (Ahn *et al.*, 2007). One possible explanation for this voltage independence is that the pK_a value of rosiglitazone is 6.1–6.8, and at least 90% of rosiglitazone is in the uncharged form at physiological pH. However, we cannot completely rule out the possibility that some of the effects described in the present study resulted from acceleration of the intrinsic inactivation of K_v4.3 channels.

Use dependence of a drug may be accomplished by the binding of the drug either to the open or inactivated states of channels (Courtney, 1975; Butterworth and Strichartz, 1990; Wang *et al.*, 1995). In terms of kinetics, use-dependent inhibition reflects a slow association rate during depolarization and a slow dissociation rate upon repolarization (Slawsky and Castle, 1994). In the present study, rosiglitazone did not cause use-dependent inhibition. The much higher dissociation rate constant of rosiglitazone caused rapid release of the drug from its binding sites on the K_v4.3 channels, which presumably contributed to the absence of use-dependent inhibition of the K_v4.3 channels (Wang *et al.*, 1995). In addition, the rapid dissociation of rosiglitazone from the K_v4.3 channels might also account for the lack of effect on the time course of recovery from inactivation (Castle, 1990). This result suggests that the rate of recovery from intrinsic inactivation of the K_v4.3 channels is similar to that of recovery from channel blocking. In the present study, rosiglitazone did not alter the time course of the tail currents of the K_v4.3 channels. The tail current crossover phenomenon, which has been reported previously for open-channel block (Snyders *et al.*, 1992), was not observed for rosiglitazone block of the K_v4.3 channels. The lack of change in deactivation kinetics of K_v4.3 channels might indicate that 'unblocking' of the channel was not necessary for channel closing and the drug could be trapped in the deactivated channels. This phenomenon is similar to the situations described for other open channel block of K_v4.3 and K_v1.5 channels (Lacerda *et al.*, 1997; Kim *et al.*, 2007).

Another characteristic of the rosiglitazone-induced inhibition of K_v4.3 channels was the hyperpolarizing shift in the steady-state inactivation and the acceleration of closed-state inactivation. K_v4.3 channels do not follow typical N-type or C-type inactivation, but depend on the concerted action of the cytoplasmic N- and C-termini (Jerng and Covarrubias, 1997). K_v4.3 channels in the open state can be inactivated at a depolarizing voltage, and these channels can also be inactivated directly from the closed state without activation at subthreshold membrane potential (Beck and Covarrubias, 2001). Therefore, the inhibitory effects of rosiglitazone could be determined from the state of the K_v4.3 channels, which depends on the holding potentials. Because the closed-state inactivation of K_v4.3 channels dominates inactivation from the open state during depolarizing pre-pulses near the $V_{1/2}$ of steady-state inactivation, the hyperpolarizing shift in the steady-state curve resulted from closed-state inactivation superimposed on the steady-state inactivation in the subthreshold range of depolarization.

Because activation of PPARγ results in very complex biological effects, we cannot exclude the possibility that rosiglitazone inhibited the K_v4.3 channels via a PPARγ-dependent mechanism. To our knowledge, there is only one report regarding the direct effects of PPARγ on ion channels: a study of voltage-gated Ca^{2+} currents in cultured hippocampal neurons, which were suppressed by thiazolidinediones via a PPARγ-dependent pathway (Pancani *et al.*, 2009). In their study, however, the neurons were treated for 24 h with the thiazolidinedione to evaluate the effects of the drug. Therefore, it is unlikely that the effect of rosiglitazone were mediated by the activation of PPARγ since we tested rosiglitazone for a short period of time (maximum 30 min) in whole-cell recordings.

Rosiglitazone is a widely used, oral hypoglycaemic agent, which improves insulin resistance in type 2 diabetes. The mechanism of action of this drug is not clear, but binding of rosiglitazone to PPARγ enhances the expression of glucose transporters in adipocytes and increases the insulin sensitivity of target tissues (Lehmann *et al.*, 1995; Wagstaff and Goa, 2002). It is generally accepted that K_v4.3 channels contribute to the transient outward K^+ current in the human heart (Ohya *et al.*, 1997). These channels display rapid activation and inactivation, and influence the early phase of cardiac action potentials, which in turn affects all currents that are subsequently activated (Dixon *et al.*, 1996). Therefore, K_v4.3 channels influence the overall duration of the action potential and regulate the excitability of cardiac myocytes. Since K_v4.3 channels are present in both the atria and ventricles, inhibition of K_v4.3 channels prolonged the action potential duration and increased the refractory period in cardiac myocytes. Accordingly, it is postulated that this channel constitutes a molecular target that is involved in the antiarrhythmic action of drugs (Wulff *et al.*, 2009). Indeed, beyond the antidiabetic activity of rosiglitazone, a remarkable improvement in paroxysmal atrial fibrillation has also been reported after rosiglitazone therapy (Korantzopoulos *et al.*, 2008). In heart failure and ischaemia, however, reduced activity of K_v4.3 channels was correlated with a decreased transient outward K^+ current and prolongation of the action potential of ventricular myocytes, providing a molecular explanation for the increased QT interval and cardiac pro-arrhythmic effect (Kaab *et al.*, 1998; Kass and Cabo, 2000). Although rosiglitazone is considered a relatively safe drug, chronic rosiglitazone treatment is associated with a significant increase in the risk of myocardial infarction and heart failure (Singh *et al.*, 2007a). Acute myocardial ischaemia appears to be an important cause of cardiac arrhythmias in humans (Janse and Wit, 1989). In some pathological conditions, such as cardiac ischaemia, the membrane potential of the cardiac myocytes is more depolarized (Lehmann-Horn and Rudel, 1995), which could increase the fraction of open- and closed-inactivated K_v4.3 channels. Thus, the inhibition of K_v4.3 channels by rosiglitazone, which occurs during depolarization in myocardial ischaemia, might have a pro-arrhythmic effect. In addition, rosiglitazone at clinically relevant doses blocked cardiac K_{ATP} channels, and this blockade of K_{ATP} channels in myocardial ischaemia can have either pro- or anti-arrhythmic effects (Lu *et al.*, 2008). The therapeutic plasma concentrations of rosiglitazone in patients with diabetes are in the range of 0.7–1.7 μM (Izumi *et al.*, 1996; Wagstaff and Goa, 2002). In the present study,

rosiglitazone inhibited the open state of K_v4.3 channels in a concentration-dependent manner with an IC_{50} value of 24.5 μM, which is comparable with the IC_{50} reported in our previous study of K_v1.3 channels (18.6 μM) expressed in CHO cells (Ahn *et al.*, 2007). These concentrations are above the therapeutic range observed clinically after oral administration of the drug. However, the K_i of 1.49 μM for the inactivated K_v4.3 channels, which was obtained from the concentration-dependent shift in the steady-state inactivation curves, could be of clinical relevance. Moreover, the higher affinity of rosiglitazone for the inactivated state of K_v4.3 channels allows this drug to inhibit K_v4.3 channel current in ischaemic tissue to a much greater extent than in normal tissue.

In conclusion, rosiglitazone potently inhibited currents carried by K_v4.3 channels in a manner consistent with both open-channel block and acceleration of the closed-state inactivation. Taken together, our results provide, at least in part, a potential explanation for the cardiovascular events observed in patients during rosiglitazone therapy.

Acknowledgements

We thank Dr Yuji Imaizumi (Department of Molecular and Cellular Pharmacology, Nagoya City University, Nagoya, Japan) for the K_v4.3 cDNA. This work was supported by a grant from the Medical Research Center, Korea Science and Engineering Foundation, Republic of Korea (R13-2002-005-01002-0).

Conflict of interest

None.

References

Ahn HS, Kim SE, Jang HJ, Kim MJ, Rhie DJ, Yoon SH *et al.* (2006). Interaction of riluzole with the closed inactivated state of Kv4.3 channels. J Pharmacol Exp Ther 319: 323–331.

Ahn HS, Kim SE, Jang HJ, Kim MJ, Rhie DJ, Yoon SH *et al.* (2007). Open channel block of Kv1.3 by rosiglitazone and troglitazone: Kv1.3 as the pharmacological target for rosiglitazone. Naunyn Schmiedebergs Arch Pharmacol 374: 305–309.

Alexander SPH, Mathie A, Peters JA (2009). Guide to Receptors and Channels (GRAC), 4th edn. Br J Pharmacol 158 (Suppl. 1): S1–S254.

Bean BP, Cohen CJ, Tsien RW (1983). Lidocaine block of cardiac sodium channels. J Gen Physiol 81: 613–642.

Beck EJ, Covarrubias M (2001). Kv4 channels exhibit modulation of closed-state inactivation in inside-out patches. Biophys J 81: 867–883.

Butterworth JFT, Strichartz GR (1990). Molecular mechanisms of local anesthesia: a review. Anesthesiology 72: 711–734.

Castle NA (1990). Bupivacaine inhibits the transient outward K^+ current but not the inward rectifier in rat ventricular myocytes. J Pharmacol Exp Ther 255: 1038–1046.

Courtney KR (1975). Mechanism of frequency-dependent inhibition of sodium currents in frog myelinated nerve by the lidocaine derivative GEA. J Pharmacol Exp Ther 195: 225–236.

Demo SD, Yellen G (1991). The inactivation gate of the Shaker K^+ channel behaves like an open-channel blocker. Neuron 7: 743–753.

Dixon JE, Shi W, Wang HS, McDonald C, Yu H, Wymore RS *et al.* (1996). Role of the Kv4.3 K^+ channel in ventricular muscle. A molecular correlate for the transient outward current. Circ Res 79: 659–668.

Fujiwara T, Horikoshi H (2000). Troglitazone and related compounds: therapeutic potential beyond diabetes. Life Sci 67: 2405–2416.

Izumi T, Enomoto S, Hosiyama K, Sasahara K, Shibukawa A, Nakagawa T *et al.* (1996). Prediction of the human pharmacokinetics of troglitazone, a new and extensively metabolized antidiabetic agent, after oral administration, with an animal scale-up approach. J Pharmacol Exp Ther 277: 1630–1641.

Janse MJ, Wit AL (1989). Electrophysiological mechanisms of ventricular arrhythmias resulting from myocardial ischemia and infarction. Physiol Rev 69: 1049–1169.

Jeck C, Pinto J, Boyden P (1995). Transient outward currents in subendocardial Purkinje myocytes surviving in the infarcted heart. Circulation 92: 465–473.

Jerng HH, Covarrubias M (1997). K^+ channel inactivation mediated by the concerted action of the cytoplasmic N- and C-terminal domains. Biophys J 72: 163–174.

Kaab S, Dixon J, Duc J, Ashen D, Nabauer M, Beuckelmann DJ *et al.* (1998). Molecular basis of transient outward potassium current downregulation in human heart failure: a decrease in Kv4.3 mRNA correlates with a reduction in current density. Circulation 98: 1383–1393.

Kass RS, Cabo C (2000). Channel structure and drug-induced cardiac arrhythmias. Proc Natl Acad Sci USA 97: 11683–11684.

Kim SE, Ahn HS, Choi BH, Jang HJ, Kim MJ, Rhie DJ *et al.* (2007). Open channel block of A-type, Kv4.3, and delayed rectifier K^+ channels, Kv1.3 and Kv3.1, by sibutramine. J Pharmacol Exp Ther 321: 753–762.

Knock GA, Mishra SK, Aaronson PI (1999). Differential effects of insulin-sensitizers troglitazone and rosiglitazone on ion currents in rat vascular myocytes. Eur J Pharmacol 368: 103–109.

Korantzopoulos P, Kokkoris S, Kountouris E, Protopsaltis I, Siogas K, Melidonis A (2008). Regression of paroxysmal atrial fibrillation associated with thiazolidinedione therapy. Int J Cardiol 125: e51–e53.

Lacerda AE, Roy ML, Lewis EW, Rampe D (1997). Interactions of the nonsedating antihistamine loratadine with a Kv1.5-type potassium channel cloned from human heart. Mol Pharmacol 52: 314–322.

Lehmann JM, Moore LB, Smith-Oliver TA, Wilkison WO, Willson TM, Kliewer SA (1995). An antidiabetic thiazolidinedione is a high affinity ligand for peroxisome proliferator-activated receptor γ (PPARγ). J Biol Chem 270: 12953–12956.

Lehmann-Horn F, Rudel R (1995). Hereditary nondystrophic myotonias and periodic paralyses. Curr Opin Neurol 8: 402–410.

Lu L, Reiter MJ, Xu Y, Chicco A, Greyson CR, Schwartz GG (2008). Thiazolidinedione drugs block cardiac K_{ATP} channels and may increase propensity for ischaemic ventricular fibrillation in pigs. Diabetologia 51: 675–685.

Mishra SK, Aaronson PI (1999). Differential block by troglitazone and rosiglitazone of glibenclamide-sensitive K^+ current in rat aorta myocytes. Eur J Pharmacol 386: 121–125.

Nissen SE, Wolski K (2007). Effect of rosiglitazone on the risk of myocardial infarction and death from cardiovascular causes. N Engl J Med 356: 2457–2471.

Ohya S, Tanaka M, Oku T, Asai Y, Watanabe M, Giles WR *et al.* (1997). Molecular cloning and tissue distribution of an alternatively spliced variant of an A-type K^+ channel alpha-subunit, Kv4.3 in the rat. FEBS Lett 420: 47–53.

Pancani T, Phelps JT, Searcy JL, Kilgore MW, Chen KC, Porter NM *et al.* (2009). Distinct modulation of voltage-gated and ligand-gated Ca^{2+} currents by PPAR-γ agonists in cultured hippocampal neurons. J Neurochem 109: 1800–1811.

Patel SP, Parai R, Campbell DL (2004). Regulation of Kv4.3 voltage-dependent gating kinetics by KChIP2 isoforms. J Physiol 557: 19–41.

Singh S, Loke YK, Furberg CD (2007a). Long-term risk of cardiovascular events with rosiglitazone: a meta-analysis. JAMA 298: 1189–1195.

Singh S, Loke YK, Furberg CD (2007b). Thiazolidinediones and heart failure: a teleo-analysis. Diabetes Care 30: 2148–2153.

Slawsky MT, Castle NA (1994). K^+ channel blocking actions of flecainide compared with those of propafenone and quinidine in adult rat ventricular myocytes. J Pharmacol Exp Ther 269: 66–74.

Snyders DJ, Yeola SW (1995). Determinants of antiarrhythmic drug action. Electrostatic and hydrophobic components of block of the human cardiac hKv1.5 channel. Circ Res 77: 575–583.

Snyders J, Knoth KM, Roberds SL, Tamkun MM (1992). Time-, voltage-, and state-dependent block by quinidine of a cloned human cardiac potassium channel. Mol Pharmacol 41: 322–330.

Wagstaff AJ, Goa KL (2002). Rosiglitazone: a review of its use in the management of type 2 diabetes mellitus. Drugs 62: 1805–1837.

Wang Z, Fermini B, Nattel S (1995). Effects of flecainide, quinidine, and 4-aminopyridine on transient outward and ultrarapid delayed rectifier currents in human atrial myocytes. J Pharmacol Exp Ther 272: 184–196.

Wulff H, Castle NA, Pardo LA (2009). Voltage-gated potassium channels as therapeutic targets. Nat Rev Drug Discov 8: 982–1001.